Received April 21, 2021, accepted May 4, 2021, date of publication May 10, 2021, date of current version May 27, 2021.

Digital Object Identifier 10.1109/ACCESS.2021.3078504

Air-Core Ring Fiber Guiding >400 Radially Fundamental OAM Modes Across S + C + L Bands

YINGNING WANG[1], WENQIAN ZHAO[1], WENPU GENG[1], YUXI FANG[1], CHANGJING BAO[2], ZHI WANG[1], HAO ZHANG[1], YONGXIONG REN[2], ZHONGQI PAN[3], (Senior Member, IEEE), AND YANG YUE[1], (Member, IEEE)

[1]Institute of Modern Optics, Nankai University, Tianjin 300350, China
[2]Department of Electrical Engineering, University of Southern California, Los Angeles, CA 90089, USA
[3]Department of Electrical and Computer Engineering, University of Louisiana at Lafayette, Lafayette, LA 70504, USA

Corresponding author: Yang Yue (yueyang@nankai.edu.cn)

This work was supported in part by the National Key Research and Development Program of China under Grant 2019YFB1803700, in part by the Key Technologies Research and Development Program of Tianjin under Grant 20YFZCGX00440, and in part by the Fundamental Research Funds for the Central Universities, Nankai University, under Grant 63201178 and Grant 63191511.

ABSTRACT In this paper, we propose and design a Ge-doped air-core ring fiber, which can support a large amount of OAM modes for mode-division multiplexing (MDM) in optical fiber communications. By varying the mole fraction of GeO_2 and adjusting the structure parameter, including the air-core radius and the GeO_2-doped ring width, we investigate the influence of different fiber parameters on the total supported OAM mode number. The hollow silica fiber with a 50-μm air core and a 1.5-μm thickness of Ge-doped ring is designed in simulation to support fiber eigenmodes up to $HE_{112,1}$ and $EH_{107,1}$. This provides 436 OAM modes at 1550 nm while maintaining radially single mode condition. Moreover, it can support more than 400 radially fundamental OAM modes for the wavelength from 1460 nm to 1625 nm, covering entire S, C and L bands. The optical parameters of the guided OAM modes in the fiber are also numerically analyzed, including effect of material loss, optical field distribution, effective refractive index profile and chromatic dispersion, etc. The simulation results show that the higher-order OAM modes have longer 2π and 10-ps walk-off length in the air-core ring fiber with ellipticity or bending compared with low-order modes.

INDEX TERMS Orbital angular momentum, fiber optics, ring fiber, multiplexing.

I. INTRODUCTION

Orbital angular momentum (OAM) beams associated with azimuthal phase dependence of the complex electric field have gained tremendous interest in recent years. It can potentially facilitate a variety of applications, such as micromanipulation [1], [2], imaging [3], [4], laser material processing [5], [6] and sensing [7], [8]. An OAM-carrying beam, which can be described in the spatial phase form of $\exp(il\varphi)$ ($l = 0, \pm1, \pm2, \ldots$), has a doughnut shaped intensity profile due to its twisted helical phase front. The amount of $2l\pi$ phase shift that occurs in the azimuthal direction represents different states or modes, which are orthogonal to each other while propagating coaxially. Consequently, they are completely independent to other multiplexing dimensions, such as wavelength and polarization, in tradition optical communication systems, thus can create an additional set of data carriers by mode-division multiplexing (MDM) system, to further improve the transmission rate and spectrum efficiency [9]–[11]. There are also some other ways of multiplexing modes in optical fibers, such as LP modes [12]–[14] and supermodes [15]–[17]. However, they require multiple-input multiple-output (MIMO) technology with high complexity. OAM modes couple less than LP modes do, lessening the need for MIMO processing [18].

Efficiently maintaining the OAM modes in an optical fiber is of great importance. However, compared with linearly polarized (LP) modes, OAM modes are unable to propagate steadily in a conventional fiber as unwanted radially higher-order modes will be excited and can be easily coupled to each other. Ring fiber could potentially maintain stable OAM modes during propagation. Since OAM modes have

The associate editor coordinating the review of this manuscript and approving it for publication was Maged Abdullah Esmail.

similar annular shape profiles as the ring fiber, they can be effectively preserved when propagating in the ring fiber. Due to this unique characteristic, ring-shaped high-index fiber has been proposed to stably guide and transmit OAM modes [19]–[26]. In recent years, lots of researches propose and experimentally demonstrate that the ring fiber with a hollow air-core can support more OAM modes because of its improved index contrast between the high-index ring and core regions of the fiber [27], [28]. A laudable goal would be to further increase the number of guided OAM modes by properly designing the ring fiber. The reach and stability of OAM mode propagation in the ring fiber can potentially provide an effective avenue for a host of different applications. In our previous research, an air-core As_2S_3 ring fiber is introduced for supporting numerous OAM modes [29] and OAM supercontinuum generation [30], [31], which is promising but challenging because the complex fabrication procedure. Compared to using As_2S_3 as high-index ring region, Ge-doped glass is more frequently used core material of telecommunication optical fiber, as its many excellent physical properties are close to silica glass.

In this paper, we design and numerically analyze an air-core GeO_2-doped ring fiber for supporting numerous OAM modes. By varying the mole fraction of GeO_2 and optimizing the structure parameter, the mode properties and propagation effects of OAM modes in the proposed fiber are numerically analyzed. The simulation results show that the designed fiber with 50-μm air-core radius and 1.5-μm ring width can simultaneously support 436 radially fundamental OAM modes at 1550 nm. Meanwhile, more than 400 OAM modes can be supported across S, C, and L bands (from 1460 nm to 1625 nm). Moreover, the characteristics of the optical field distribution, effective refractive index profile and chromatic dispersion are also calculated for supported OAM modes in the fiber. The results show that this design could ensure the large effective index difference between the adjacent modes, improving the stability of the OAM modes transmission. Besides, the effective refractive index difference of even and odd fiber eigenmodes induced by the fiber ellipticity or bending, and their impacts on the walk-off length are carefully analyzed. Compared to low-order OAM modes, the higher order OAM modes are more tolerant to these fiber variations. The proposed fiber could represent a promising avenue for increasing the transmission capacity in optical OAM-based communications systems.

II. DESIGN OF THE GE-DOPED AIR-CORE FIBER

Here, the designed fiber we propose has a hollow air-core as a repulsive barrier and a high-index Ge-doped ring region as the transport layer to guide the OAM modes. Figure 1(a) illustrates the concept of OAM mode multiplexing, which is a process of transmitting multiple OAM modes in the designed air-core ring fiber simultaneously, representing the OAM modes with different l states are multiplexed. The cross section and the refractive index profile of the proposed fiber are shown in Figure 1(b). The air-core used here can force

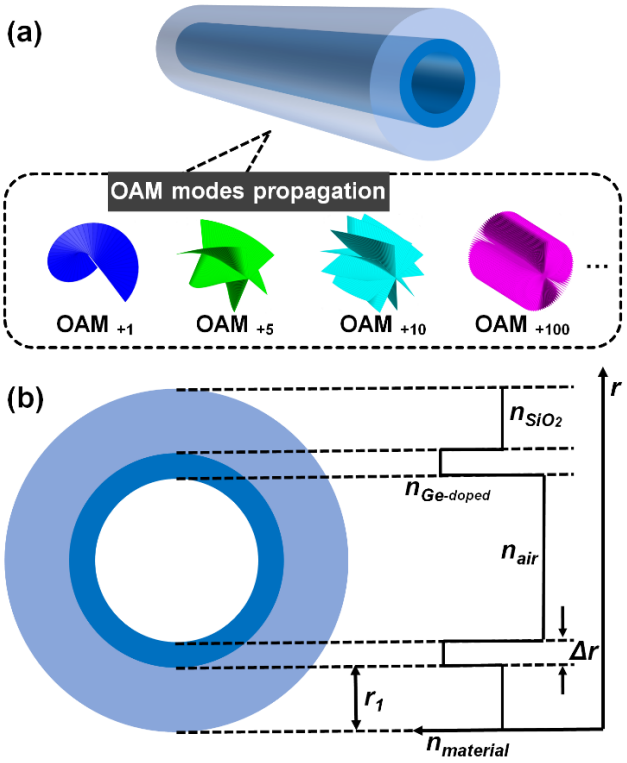

FIGURE 1. (a) Concept of OAM mode multiplexing; (b) Cross-section of the Ge-doped air-core ring fiber and index profile of three waveguide layers.

the mode field to encounter the large index contrast between the high-index ring and the outer cladding [27]. Moreover, a 125-μm fiber cladding diameter is chosen, which is the same as the standard single-mode optical fiber (SMF). This structure could significantly reduce the intermodal coupling by increasing the mode effective refractive index difference. From the fabrication point of view, the material selection and fiber structure design are feasible as the fiber with solid cladding and a high refractive index germanium doped silica ring core has been manufactured in practice [21], which can be performed by using the modified chemical vapor deposition (MCVD) method [32], [33].

III. MODE PROPERTY

A. EFFECT OF GeO_2 CONCENTRATION

In the practical application, preserving only the radially fundamental OAM modes in the designed fiber could significantly help avoid the crosstalk of the first radial order and the higher radial order OAM modes, simplifying the processes of multiplexing and demultiplexing [34]–[36]. We investigate the relationship between different mole fraction of GeO_2 and the ring width (Δr), while maintaining single-radial mode condition. One can see from Figure 2(a), as the mole fraction of GeO_2 decreases, the range of ring width to maintain single-radial mode condition becomes more adjustable. The largest ring widths of the fiber for 50 mol.%, 80 mol.% and 100 mol.% fractions of GeO_2 are 1.5 μm, 1.7 μm and 2.2 μm, corresponding to the material refractive indices at 1550 nm

are 1.5173, 1.5596 and 1.5871, respectively. The material refractive indices of Ge-doped silica are obtained by using the Sellmeier equations in our model [37], [38].

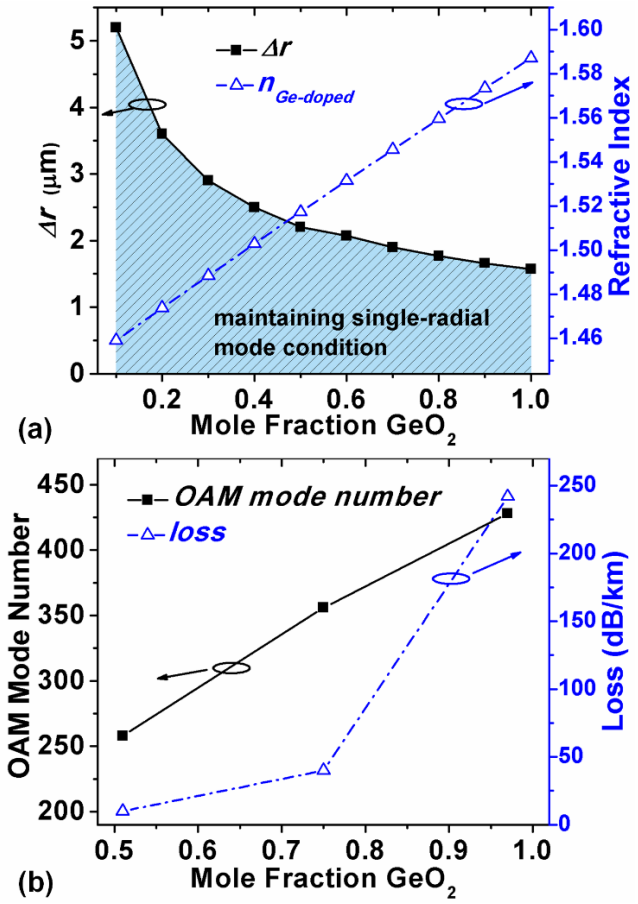

FIGURE 2. (a) The ring width (Δr) of the designed fiber to maintain single-radial mode condition and corresponding material refractive index of the ring region as a function of different mole fraction of GeO_2; (b) OAM mode number and loss of GeO_2-based fiber from [30] as a function of different mole fraction of GeO_2.

Figure 2(b) depicts the relationship between OAM mode number and optical-loss from different concentration categories at 1550 nm. According to the research, the fiber with 51, 75, and 97 mol.% GeO_2 can supported 258, 356 and 428 OAM mode number, while the corresponding optical-loss are about 10, 40 and 242 dB/km at 1550 nm, respectively. Consequently, the trade-off between the material loss and the supported mode numbers should be considered on the basis of fiber's different applications, in which the fiber with higher mole fractions of GeO_2 can support more OAM modes but the fiber's optical loss also grows up [39].

B. SUPPORTED OAM MODE NUMBER

Full-vector finite-element-method (FEM) is a popular choice for numerical modeling optical fiber properties, such as effective refractive index, loss, dispersion, effective area, and so on. We then investigate the supported OAM mode number variations in the designed Ge-doped air-core ring fiber as a function of different air-core radii (r_1) with different mole

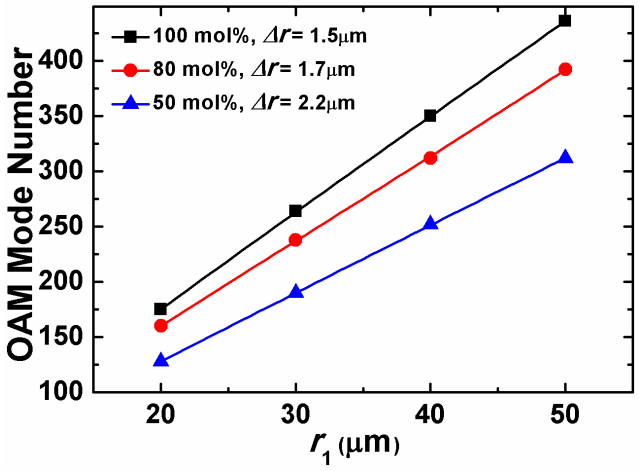

FIGURE 3. OAM mode number in the designed ring fiber as a function of the air-core radius (r_1) with different mole fraction of GeO_2.

fraction by FEM as shown in Figure 3. The largest ring width is chosen under the condition of fiber with different mole fraction. One can consider that possible design with large r_1 can increase the supported OAM mode number, which is mainly due to that larger air-core radius has more radial space to support more fiber eigenmodes. The Ge-doped air-core ring fiber with parameters of $r_1 = 50\ \mu$m and $\Delta r = 1.5\ \mu$m can support the eigenmodes up to $HE_{112,1}$ and $EH_{107,1}$ at 1550 nm, i.e. 436 OAM modes in total. Furthermore, the increase of GeO_2 concentration can further increase the number of supported OAM modes due to larger material index-contrast, but with sacrificed fiber loss according to the foregoing result.

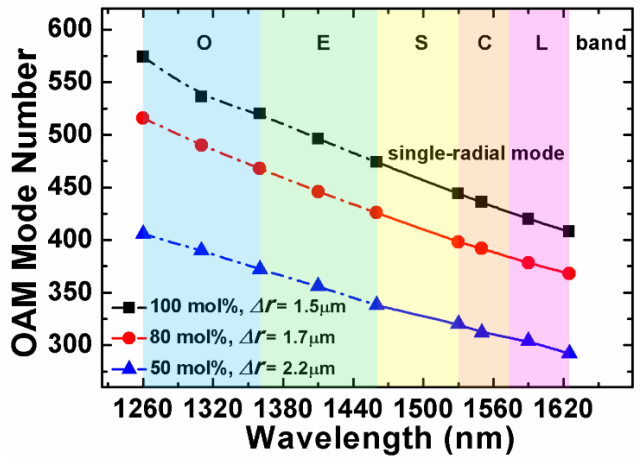

FIGURE 4. OAM mode number of the designed fiber with $r_1 = 50\ \mu$m as a function of wavelength with different mole fraction of GeO_2.

The supported OAM mode number as a function of wavelength with different mole fraction of GeO_2 in the designed fiber with $r_1 = 50\ \mu$m is checked in Figure 4. The solid line corresponds to the result of maintaining only the single-radial OAM mode. On the other hand, the dot line represents that the unwanted radially second-order OAM modes appear. For the designed fibers with different mole fractions of GeO_2

under the largest ring width, the radially high-order modes all appear from 1460 nm to shorter wavelength. We found that numerous OAM modes would be provided across S, C, and L-band for the designed fiber with $r_1 = 50$ μm and 100 mol.% fractions of GeO_2 in the single-mode condition of radial direction, which linearly decrease with wavelength and reach the minimum to about 400 at 1625 nm. Besides, the fiber with $r_1 = 50$ μm and 50 mol.% mole fractions of GeO_2 is expected to support up to approximately 300 radially fundamental OAM modes across S, C, and L-band ranged from 1460 nm to 1625 nm. Though the supported OAM mode numbers for the proposed fiber in the short wavelength are very high, it will lose the radially single-mode condition.

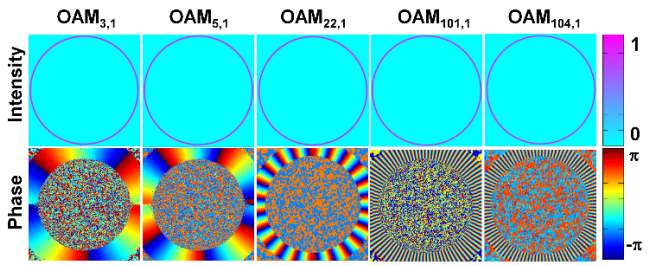

FIGURE 5. The normalized intensity and phase distribution of the $OAM_{3,1}$, $OAM_{5,1}$, $OAM_{22,1}$, $OAM_{101,1}$, $OAM_{104,1}$ modes in the air-core ring fiber ($r_1 = 50$ μm, $\Delta r = 1.5$ μm).

For the ring fiber with $r_1 = 50$ μm and 100 mol.% mole fractions of GeO_2 across C and L bands from 1530 nm to 1625 nm, 436 OAM modes can be supported by $HE_{m,1}$ and $EH_{n,1}$ ($m = 2 \sim 105$, $n = 1 \sim 100$). The property of the EH modes are closer to that of the TM mode, while the characteristics of the HE mode are closer to that of the TE mode. For example, the electric field lines of the TM mode radiate outward from the center, so is the one of the EH mode. Consequently, we can distinguish HE and EH eigenmodes from their electric field distributions. As an example, Figure 5 depicts the simulation of the normalized intensity profiles and the phase distributions for some $OAM_{l,1}$ modes ($HE_{4,1}$, $HE_{6,1}$, $HE_{23,1}$, $EH_{100,1}$ and $HE_{105,1}$ correspond to $OAM_{3,1}$, $OAM_{5,1}$, $OAM_{22,1}$, $OAM_{101,1}$, $OAM_{104,1}$ modes, respectively) in the fiber, which are made up by the even and odd eigenmodes ($OAM^{\pm}_{\pm l,1} = HE^{even}_{l+1,1} \pm jHE^{odd}_{l+1,1}$, $OAM^{\mp}_{\pm l,1} = EH^{even}_{l-1,1} \pm jEH^{odd}_{l-1,1}$). For OAM mode with $|l| = 1$, there are $OAM^{\pm}_{\pm 1,1} = HE^{even}_{2,1} \pm jHE^{odd}_{2,1}$ and $OAM^{\mp}_{\pm 1,1} = TM^{even}_{0,1} \pm jTE^{odd}_{0,1}$. However, $TM_{0,1}$ and $TE_{0,1}$ mode supported in this structure cannot degenerate into a stable OAM mode due to large propagation constant difference. The shape of the ring-like intensity distribution still remains and well-confined in the ring fiber. Moreover, the phase distribution of the $OAM_{l,1}$ mode shows a $2l\pi$ change azimuthally, which provides a chance to efficiently demultiplex these OAM modes with different orders by using a conjugate phase pattern.

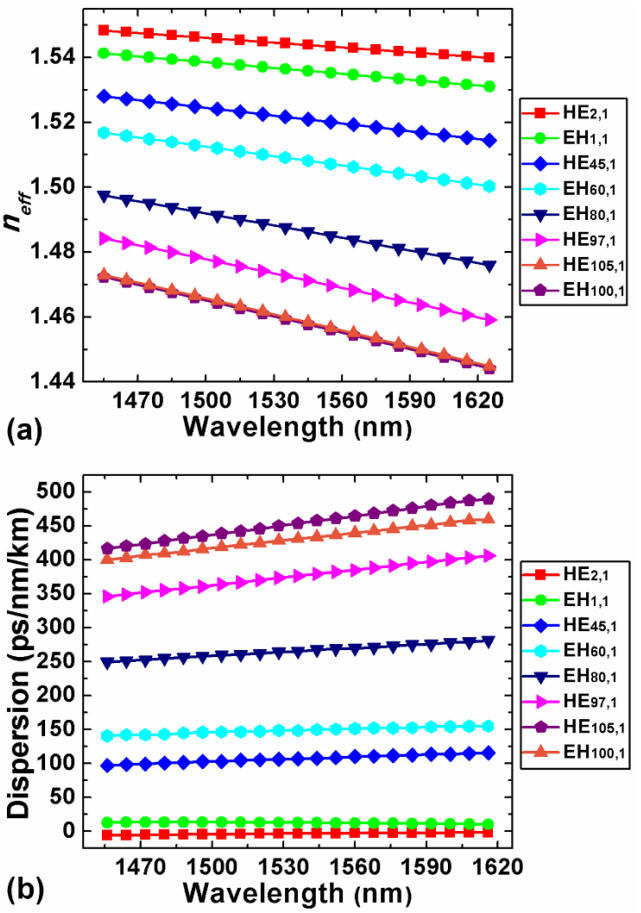

FIGURE 6. (a) Effective refractive index and (b) dispersion of the designed fiber with parameters of $r_1 = 50$ μm and $\Delta r = 1.5$ μm as a function of wavelength for different vortex modes.

C. OPTICAL PROPERTIES IN S + C + L BANDS

The effective index and chromatic dispersion are studied to assess the MDM application capability in the S, C, and L band and the simulation results are summarized in Figure 6. The effective refractive indices (n_{eff}) of some OAM modes supported in the air-core ring fiber with fiber parameters of $r_1 = 50$ μm and 100 mol.% mole fractions of GeO_2 over S, C and L bands are illustrated in Figure 6(a). All the effective indices of the OAM modes can only be packed somewhere between the refractive index of the silica cladding and the refractive index of the high-index Ge-doped ring. Furthermore, higher-order mode has a lower effective refractive index than the lower-order mode. We can also observe that n_{eff} of the eigenmodes monotonously decrease with the wavelength. The effective index difference between the $HE_{l+1,1}$ and $EH_{l-1,1}$ modes in a group of $OAM_{l,1}$ should be maintained above 10^{-4} to assure the good separation and preclude linearly polarized (LP) mode formation according to the previous researches [21]. From the calculated results, the condition is more achievable for the lower topological charge. For the lowest-order mode $|l| = 1$ family, the $HE_{3,1}$ and $EH_{1,1}$ mode have enough index difference with about 10^{-2} separation. Furthermore, the lowest effective index

difference between $HE_{102,1}$ and $EH_{100,1}$ within $|l| = 101$ family can reach to approximately 6.3×10^{-4} conducing the stable transmission of OAM modes across the whole S, C and L bands.

Dispersion is an effect that can spread the light pulse in the time domain, which can decrease the performance of a signal transmitted in the optical fiber. It is usually composed by two sources of dispersion including waveguide dispersion and material dispersion. The following simulation results show the total dispersion including the waveguide and material dispersions. The dispersion characteristics of the eigenmodes that form OAM modes in the air-core ring fiber with 50-μm r_1 and 100 mol.% mole fractions of GeO_2 are shown in Figure 6(b). Noted that the $HE_{2,1}$ and $EH_{1,1}$ modes feature low dispersion (−4.133 ps/nm/km and 14.467 ps/nm/km) at 1550 nm and small dispersion variations (<3.958 ps/nm/km and 3.294 ps/nm/km) across S, C and L bands, while the chromatic dispersion increases to more than 400 ps/nm/km as the mode order becomes higher. Although the chromatic dispersion of some high-order OAM mode is very large, we expect that they could be compensated by OAM dispersion compensating fiber (DCF), which have large negative dispersion [36], [40] and digital signal processing (DSP) in the coherent transmission systems according to the previous studies [41].

D. FIBER ELLIPTICITY AND BENDING

In the practical fiber optics communication, OAM modes are sensitive to some perturbations imposed on the ring fiber, such as stress, strain and twist which can lead to fiber deformation. Therefore, the nonperfect circularity (ellipticity) and fiber bends resulting from transmission environment will deteriorate the OAM modes transmitted in the optical fiber-based system. Ellipticity and bending of the fiber will cause a difference to the propagation constants of the even and odd modes for $HE_{l-1,1}$ or $EH_{l+1,1}$, which form the $OAM_{l,1}$ mode and thus affect the mode profile and purity of OAM modes.

The ellipticity and bending effects on the proposed fiber are calculated for the effective refractive index difference of the even and odd fiber eigenmodes which compose OAM modes as shown in Figure 7. We note that the fiber ellipticity and bending have a mirror effect on the characteristics of the high-order modes. This is mainly because that more azimuthal periods in the high-order OAM modes' transverse field distribution could help mitigating the influence from fiber deformation. Figure 7(a) shows that the effective refractive index difference of $EH_{1,1}$ mode increase from about 10^{-6} to 10^{-4} as the ellipticity of air-core ring fiber increases from 0.1% to 2%. For high-order OAM modes (composed by the even and odd modes of $EH_{100,1}$ and $HE_{105,1}$), the effective refractive index differences are always around 1×10^{-10}. The effective refractive index differences of both $HE_{2,1}$ and $EH_{1,1}$ modes increase about 60 times with bending radius $r = 30$ mm compared to straight fiber as shown in Figure 7(b). The effective refractive index differences of

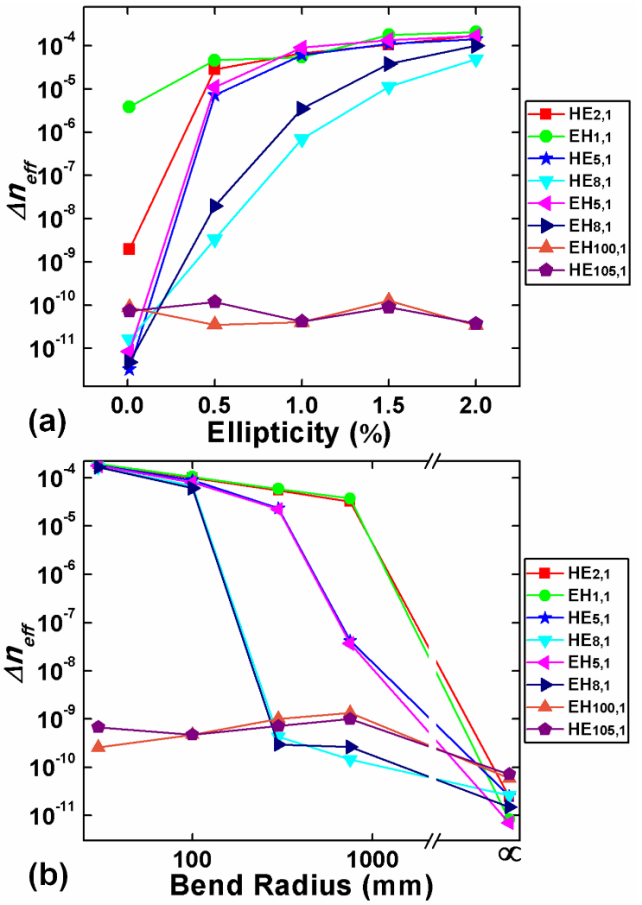

FIGURE 7. The effective refractive index differences as functions of (a) ellipticity and (b) bend radius of the designed fiber with $r_1 = 50$ μm and $\Delta r = 1.5$ μm for some OAM modes.

the high-order OAM modes can keep stable in any bending environment for bending radius up to 30 mm.

The temporal walk-off effect upon propagation reveals the influence of the fiber inter-modal crosstalk. Here, we calculate $L_{2\pi}$ and L_{10ps} to evaluate the intramode walk-off of the OAM modes at 1550 nm. 2π walk-off length ($L_{2\pi}$), known as the propagation length when the even and odd modes have a 2π relative phase shift, can be expressed as

$$L_{2\pi} = \frac{\lambda}{n_{eff}^{even} - n_{eff}^{odd}} = \frac{1.55 \times 10^{-6}}{n_{eff}^{even} - n_{eff}^{odd}}(m) \quad (1)$$

where λ is the wavelength, n_{eff}^{even} and n_{eff}^{odd} are the effective refractive indices of the even and odd eigenmodes, respectively. 10-ps walk-off length (L_{10ps}), to describe the propagation length when the even and odd fiber eigenmodes have a 10-ps temporal walk off, represents the impact of temporal walk-off on the signal quality. It can be characterized as

$$L_{10_{ps}} = \frac{c \times \Delta t}{n_{eff}^{even} - n_{eff}^{odd}} = \frac{3 \times 10^{-3}}{n_{eff}^{even} - n_{eff}^{odd}}(m) \quad (2)$$

where c and Δt are the vacuum velocity of light and the temporal walk-off time, respectively [13], [23].

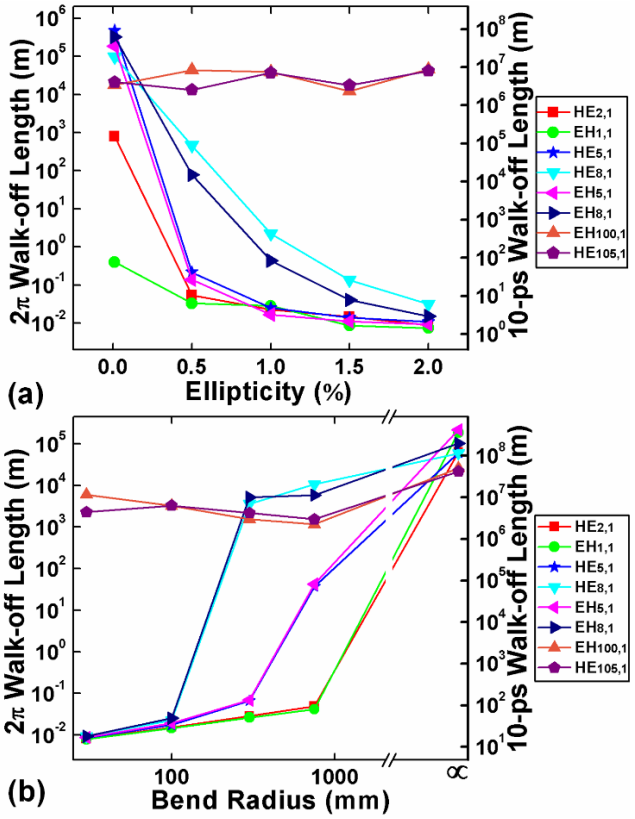

FIGURE 8. 2π and 10-ps walk-off length as functions of (a) ellipticity and (b) bend radius of the designed fiber with $r_1 = 50$ μm and $\Delta r = 1.5$ μm for some OAM modes.

The walk-off length variations of some OAM modes supported in the designed fiber with parameters of $r_1 = 50$ μm and 100 mol.% mole fractions of GeO_2 as functions of fiber ellipticity and bend radius are depicted in Figure 8(a) and (b). For the higher-order OAM modes, its smaller modal index difference ($n_{eff}^{even} - n_{eff}^{odd}$) induced by the fiber ellipticity or bending leads to a longer 2π and 10-ps walk-off length. In particular, for the highest-order OAM modes (EH100,1 and $HE_{105,1}$ corresponded $OAM_{101,1}$ and $OAM_{103,1}$ modes) can propagate more than 10^6 m with <10-ps mode walk-off, even in an air-core ring fiber with 2% ellipticity. However, for the low-order OAM modes, the modal index differences increase tremendously with the fiber ellipticity and bending, resulting in a shorter walk-off length. This means instability transmission of low-order OAM modes when suffering environmental disturbance.

E. MODE PURITY

For fibers with the large discontinuity in the refractive index profile, strong spin-orbit coupling occurs, and it will result in impure eigenmodes [42]. Here, we numerically investigate the OAM mode purity in the designed air-core fiber at the wavelength of 1550 nm, which is an important indicator to measure the stability of the supported OAM modes. The transverse components of the OAM modes in the cylindrical

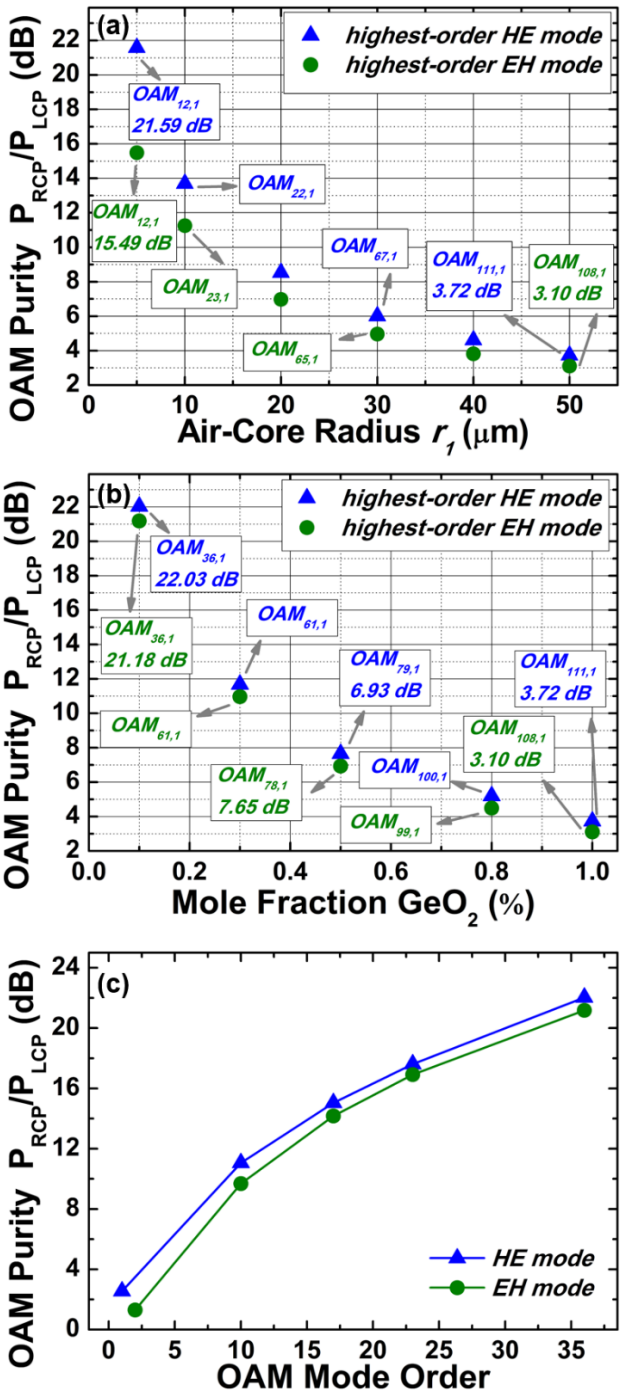

FIGURE 9. OAM mode purity as functions of (a) different air-core radius of the designed fiber with $\Delta r = 1.5$ μm and 100 mol.% GeO_2, (b) different mole fraction of GeO_2 of the designed fiber with $r_1 = 50$ μm, and (c) different OAM order of the designed fiber with $r_1 = 50$ μm and 10 mol.% GeO_2.

coordinates (r, φ) can be written as [28], [43], [44],

$$OAM_{\pm l,1}^{\pm} = f_{l+1}(r)e^{\pm il\varphi}\hat{\sigma}^{\pm} \pm g_{l+1}(r)e^{\pm i(l+2)\varphi}\hat{\sigma}^{\mp} \tag{3a}$$

$$OAM_{\pm l,1}^{\mp} = f_{l-1}(r)e^{\pm il\varphi}\hat{\sigma}^{\mp} \pm g_{l-1}(r)e^{\pm i(l-2)\varphi}\hat{\sigma}^{\pm} \tag{3b}$$

TABLE 1. Supported OAM mode number in fibers.

Fiber Type	Supported Mode Number	Reference
dual guided Schott SF_2 ring PCF	82	[45]
circular core shaped PCF	38	[46]
circular silica PCF	80	[47]
hollow core Schott SF_2 ring PCF	48	[48]
ring-based coil structure silica PCF	56	[49]
Schott multi-ring fiber	154	[50]
trench-assisted Schott multi-ring fiber	418	[23]
air-core GeO_2-doped ring fiber	436	this work

where $\hat{\sigma}^{\pm}$ means right or left polarization. Moreover, $\boldsymbol{f}_{l\pm1}(\boldsymbol{r})$ and $\boldsymbol{g}_{l\pm1}(\boldsymbol{r})$ are related to the fiber design parameters, which varies with the ring thickness and core radius. According to the equation, the dominant component is $\mathrm{OAM}_{l,1}$, while the secondary component is $\mathrm{OAM}_{l\pm2,1}$. The power ratio of the dominant component to the secondary component is called OAM polarization mode purity.

We calculate the highest-order mode purity as a function of different air-core radius of the designed fiber with 1.5-μm Δr and 100 mol.% GeO_2 as shown in Figure 9(a). Furthermore, the OAM mode purity of the designed fiber with 50-μm r_1 and 1.5-μm Δr as different mole fraction of GeO_2 are shown in Figure 9(b). One can see that larger air-core radius and higher mole fraction can support higher-order OAM modes but sacrifice the mode purity. Figure 9(c) depicts different OAM order of the designed fiber with 50-μm r_1 and 10 mol.% GeO_2. It indicates that the OAM mode purity increases with the mode order, which can be explained that the electrical fields of the higher-order modes are less confined in the ring region and thus the overlap is smaller. Another noticeable thing is that the HE-based OAM modes are universally purer than EH-based OAM modes.

IV. EVOLUTION OF OAM-CARRYING FIBERS

We compare the supported OAM mode number in this work with some previously known simulation research results of OAM-carrying fibers, which can be found in Table 1. From the table, we can obviously observe achieved OAM mode numbers with different fiber types, and our designed fiber can support more OAM modes to achieve a larger data-transmission capacity.

V. CONCLUSION

In summary, we propose and design a novel air-core GeO_2-doped ring fiber for supporting numerous OAM modes. The characteristics of the OAM modes in the proposed fiber are thoroughly analyzed by varying the mole fraction of GeO_2 and adjusting the structure parameter. Numerical analysis shows that fiber with 50-μm air-core radius and 1.5-μm ring width can simultaneously support 436 radially fundamental OAM modes at 1550 nm. Besides, we further verify by simulation that more than 400 OAM modes can be supported across all the S, C, and L bands. Moreover, the characteristics of the optical field distribution, chromatic dispersion and the effects of fiber ellipticity and bending are also analyzed numerically for different OAM beams in the designed fiber. We found that high-order OAM modes show more tolerance to the fiber ellipticity and bending caused by transmission environment.

The proposed fiber can be potentially applied in WDM, MDM, and SDM optical communications systems to tremendously increase the data-transmission capacity. With hundreds of supported OAM modes, it could theoretically provide more than 400 channels, which is also compatible with wavelength division multiplexing technique (S + C + L band) to increase thousands of times the total transmission capacity compared with a single channel. However, still additional researches are needed to further improve the channel number, insertion loss, and crosstalk for these relevant optical devices of generating and (de)multiplexing multiple OAM channels. In addition, reducing the cost and size for real-environmental OAM systems could become another considerable issue, which should be improved in the long run.

REFERENCES

[1] M. E. J. Friese, T. A. Nieminen, N. R. Heckenberg, and H. Rubinsztein-Dunlop, "Optical alignment and spinning of laser-trapped microscopic particles," *Nature*, vol. 394, no. 6691, pp. 348–350, Jul. 1998.

[2] K. Dholakia and T. Čižmár, "Shaping the future of manipulation," *Nature Photon.*, vol. 5, no. 6, pp. 335–342, Jun. 2011.

[3] A. Jesacher, M. Ritsch-Marte, and R. Piestun, "Three-dimensional information from two-dimensional scans: A scanning microscope with postacquisition refocusing capability," *Optica*, vol. 2, no. 3, pp. 210–213, 2015.

[4] G. A. Swartzlander, E. L. Ford, R. S. Abdul-Malik, L. M. Close, M. A. Peters, D. M. Palacios, and D. W. Wilson, "Astronomical demonstration of an optical vortex coronagraph," *Opt. Exp.*, vol. 16, no. 14, pp. 10200–10207, 2008.

[5] M. Duocastella and C. B. Arnold, "Bessel and annular beams for materials processing," *Laser Photon. Rev.*, vol. 6, no. 5, pp. 607–621, Sep. 2012.

[6] J. Hamazaki, R. Morita, K. Chujo, Y. Kobayashi, S. Tanda, and T. Omatsu, "Optical-vortex laser ablation," *Opt. Exp.*, vol. 18, no. 3, pp. 2144–2151, Feb. 2010.

[7] N. Cvijetic, G. Milione, E. Ip, and T. Wang, "Detecting lateral motion using Light's orbital angular momentum," *Sci. Rep.*, vol. 5, no. 1, pp. 1–7, Dec. 2015.

[8] G. Xie, H. Song, Z. Zhao, G. Milione, Y. Ren, C. Liu, R. Zhang, C. Bao, L. Li, Z. Wang, K. Pang, D. Starodubov, B. Lynn, M. Tur, and A. E. Willner, "Using a complex optical orbital-angular-momentum spectrum to measure object parameters," *Opt. Lett.*, vol. 42, no. 21, pp. 4482–4485, Nov. 2017.

[9] N. Bozinovic, Y. Yue, Y. Ren, M. Tur, P. Kristensen, H. Huang, A. E. Willner, and S. Ramachandran, "Terabit-scale orbital angular momentum mode division multiplexing in fibers," *Science*, vol. 340, no. 6140, pp. 1545–1548, Jun. 2013.

[10] A. E. Willner, H. Huang, Y. Yan, Y. Ren, N. Ahmed, G. Xie, C. Bao, L. Li, Y. Cao, Z. Zhao, J. Wang, M. P. J. Lavery, M. Tur, S. Ramachandran, A. F. Molisch, N. Ashrafi, and S. Ashrafi, "Optical communications using orbital angular momentum beams," *Adv. Opt. Photon*, vol. 7, pp. 66–106, Mar. 2015.

[11] K. Ingerslev, P. Gregg, M. Galili, F. D. Ros, H. Hu, F. Bao, M. A. U. Castaneda, P. Kristensen, A. Rubano, L. Marrucci, K. Rottwitt, T. Morioka, S. Ramachandran, and L. K. Oxenløwe, "12 mode, WDM, MIMO-free orbital angular momentum transmission," *Opt. Exp.*, vol. 26, no. 16, pp. 20225–20232, 2018.

[12] C. Xia, R. Amezcua-Correa, N. Bai, E. Antonio-Lopez, D. M. Arrioja, A. Schulzgen, M. Richardson, J. Liñares, C. Montero, E. Mateo, X. Zhou, and G. Li, "Hole-assisted few-mode multicore fiber for high-density space-division multiplexing," *IEEE Photon. Technol. Lett.*, vol. 24, no. 21, pp. 1914–1917, Nov. 13, 2012.

[13] T. Watanabe and Y. Kokubun, "Over 300 channels uncoupled few-mode multi-core fiber for space division multiplexing," in *Proc. Opt. Fiber Commun. Conf. Exhib. (OFC)*, Mar. 2014, pp. 1–3.

[14] T. Sakamoto, K. Saitoh, S. Saitoh, Y. Abe, K. Takenaga, A. Urushibara, M. Wada, T. Matsui, K. Aikawa, and K. Nakajima, "120 spatial channel few-mode multi-core fibre with relative core multiplicity factor exceeding 100," in *Proc. Eur. Conf. Opt. Commun. (ECOC)*, Sep. 2018, pp. 1–3.

[15] T. Sakamoto, T. Mori, M. Wada, T. Yamamoto, and F. Yamamoto, "Coupled multicore fiber design with low intercore differential mode delay for high-density space division multiplexing," *J. Lightw. Technol.*, vol. 33, no. 6, pp. 1175–1181, Mar. 15, 2015.

[16] S. Li and J. Wang, "Supermode fiber for orbital angular momentum (OAM) transmission," *Opt. Exp.*, vol. 23, no. 14, pp. 45–18736, Jul. 13 2015.

[17] M.-J. Li, K. Li, X. Chen, J. S. Stone, W. Xiong, J. E. Hurley, and S. C. Garner, "Multicore multimode fiber—A new type of fiber using coupled-core structures," *IEEE J. Sel. Topics Quantum Electron.*, vol. 26, no. 4, pp. 1–10, Jul. 2020.

[18] P. Genevaux, C. Simonneau, G. Labroille, B. Denolle, O. Pinel, P. Jian, J.-F. Morizur, and G. Charlet, "6-mode spatial multiplexer with low loss and high selectivity for transmission over few mode fiber," in *Proc. Opt. Fiber Commun. Conf. Exhib. (OFC)*, Mar. 2015, pp. 1–3.

[19] J. Zhang, Y. Wen, H. Tan, J. Liu, L. Shen, M. Wang, J. Zhu, C. Guo, Y. Chen, Z. Li, and S. Yu, "80-channel WDM-MDM transmission over 50-km ring-core fiber using a compact OAM DEMUX and modular 4×4 MIMO equalization," in *Proc. Opt. Fiber Commun. Conf. (OFC)*, 2019, pp. 1–3.

[20] Y. Yue, Y. Yan, N. Ahmed, J.-Y. Yang, L. Zhang, Y. Ren, H. Huang, K. M. Birnbaum, B. I. Erkmen, S. Dolinar, M. Tur, and A. E. Willner, "Mode properties and propagation effects of optical orbital angular momentum (OAM) modes in a ring fiber," *IEEE Photon. J.*, vol. 4, no. 2, pp. 535–543, Apr. 2012.

[21] C. Brunet, P. Vaity, Y. Messaddeq, S. LaRochelle, and L. A. Rusch, "Design, fabrication and validation of an OAM fiber supporting 36 states," *Opt. Exp.*, vol. 22, no. 21, pp. 26117–26127, 2014.

[22] G. Zhu, Z. Hu, X. Wu, C. Du, W. Luo, Y. Chen, X. Cai, J. Liu, J. Zhu, and S. Yu, "Scalable mode division multiplexed transmission over a 10-km ring-core fiber using high-order orbital angular momentum modes," *Opt. Exp.*, vol. 26, no. 2, pp. 594–604, 2018.

[23] S. Li and J. Wang, "A compact trench-assisted multi-orbital-angular-momentum multi-ring fiber for ultrahigh-density space-division multiplexing (19 rings×22 modes)," *Sci. Rep.*, vol. 4, no. 3853, pp. 1–8, May 2015.

[24] Y. Peng, H. Jia, and L. Fang, "Theoretical analysis of hollow ring-core optical fiber for transmitting orbital angular momentum modes," *J. Modern Opt.*, vol. 64, pp. 1–15, Oct. 2017.

[25] X. Sun, Y. Geng, Q. Zhu, X. Feng, W. Huang, Y. Zhang, W. Wang, and L. Liu, "Edge-dip air core fiber for improvement of the transmission of higher-order OAM modes," *Proc. SPIE*, vol. 2017, Mar. 2017, Art. no. 107103E.

[26] S. Ramachandran, P. Gregg, P. Kristensen, and S. E. Golowich, "On the scalability of ring fiber designs for OAM multiplexing," *Opt. Exp.*, vol. 23, no. 3, pp. 3721–3730, Feb. 2015.

[27] P. Gregg, P. Kristensen, and S. Ramachandran, "Conservation of orbital angular momentum in air-core optical fibers," *Optica*, vol. 2, no. 3, pp. 267–270, Mar. 2015.

[28] P. Gregg, P. Kristensen, A. Rubano, S. Golowich, L. Marrucci, and S. Ramachandran, "Enhanced spin orbit interaction of light in highly confining optical fibers for mode division multiplexing," *Nature Commun.*, vol. 10, no. 4707, pp. 1–8, Dec. 2019.

[29] Y. Wang, C. Bao, W. Geng, Y. Lu, Y. Fang, B. Mao, Y.-G. Liu, B. Liu, H. Huang, Y. Ren, Z. Pan, and Y. Yue, "Air-core ring fiber with >1000 radially fundamental OAM modes across O, E, S, C, and L bands," *IEEE Access*, vol. 8, pp. 68280–68287, 2020.

[30] Y. Wang, Y. Fang, W. Geng, J. Jiang, Z. Wang, H. Zhang, C. Bao, H. Huang, Y. Ren, Z. Pan, and Y. Yue, "Beyond two-octave coherent OAM supercontinuum generation in air-core As_2S_3 ring fiber," *IEEE Access*, vol. 8, pp. 96543–96549, 2020.

[31] Y. Wang, C. Bao, J. Jiang, Y. Fang, W. Geng, Z. Wang, W. Zhang, H. Huang, Y. Ren, Z. Pan, and Y. Yue, "Two-octave supercontinuum generation of high-order OAM modes in air-core As_2S_3 ring fiber," *IEEE Access*, vol. 8, pp. 114135–114142, 2020.

[32] V. M. Mashinsky, O. I. Medvedkov, V. B. Neustruev, V. V. Dvoyrin, S. A. Vasiliev, E. M. Dianov, V. F. Khopin, and A. N. Guryanov, "Germania-glass-core silica-glass-cladding MCVD optical fibres," in *Proc. Eur. Conf. Opt. Commun. (ECOC)-ICOC*, Rimini, Italy, vol. 2, Sep. 1999, pp. 210–211.

[33] A. M. Peder-Gothoni and M. Leppihalme, "GeO_2-core/SiO_2-cladding optical fibers made by MCVD process for stimulated Raman applications," *Appl. Phys. B, Lasers Opt.*, vol. 42, no. 1, pp. 45–49, Jan. 1987.

[34] L. Zhu, G. Zhu, A. Wang, L. Wang, J. Ai, S. Chen, C. Du, J. Liu, S. Yu, and J. Wang, "18 km low-crosstalk OAM+ WDM transmission with 224 individual channels enabled by a ring-core fiber with large high-order mode group separation," *Opt. Lett.*, vol. 43, no. 8, pp. 1890–1893, 2018.

[35] A. Trichili, K.-H. Park, M. Zghal, B. S. Ooi, and M.-S. Alouini, "Communicating using spatial mode multiplexing: Potentials, challenges, and perspectives," *IEEE Commun. Surveys Tuts.*, vol. 21, no. 4, pp. 3175–3203, May 2019.

[36] Z.-A. Hu, Y.-Q. Huang, A.-P. Luo, H. Cui, Z.-C. Luo, and W.-C. Xu, "Photonic crystal fiber for supporting 26 orbital angular momentum modes," *Opt. Exp.*, vol. 24, no. 15, pp. 17285–17291, Jul. 2016.

[37] E. D. Palik, *Handbook of Optical Constants of Solids*. New York, NY, USA: Academic, 1985.

[38] V. Brückner, "To the use of sellmeier formula," *Senior Experten Service Bonn HfT Leipzig Germany*, vol. 42, pp. 242–250, 2011.

[39] E. M. Dianov and V. M. Mashinsky, "Germania-based core optical fibers," *J. Lightw. Technol.*, vol. 23, no. 11, pp. 3500–3508, Nov. 1, 2005.

[40] W. Geng, Y. Li, Y. Fang, Y. Wang, C. Bao, Y. Yan, Z. Wang, W. Zhang, H. Huang, Y. Ren, Z. Pan, and Y. Yue, "Highly dispersive coupled ring-core fiber for OAM modes," *Appl. Phys. Lett.*, vol. 117, no. 19, Nov. 2020, Art. no. 191101.

[41] T. Xu, G. Jacobsen, S. Popov, J. Li, E. Vanin, K. Wang, A. T. Friberg, and Y. Zhang, "Chromatic dispersion compensation in coherent transmission system using digital filters," *Opt. Exp.*, vol. 18, no. 15, pp. 16243–16257, 2010.

[42] L. Wang, A. Corsi, L. A. Rusch, and S. LaRochelle, "Investigation of orbital angular momentum mode purity in air-core optical fibers," in *Proc. IEEE Photon. Soc. Summer Topical Meeting (SUM)*, Newport Beach, CA, USA, Jul. 2016, pp. 203–204.

[43] M. Banawan, L. Wang, S. LaRochelle, and L. A. Rusch, "Quantifying the coupling and degeneracy of OAM modes in high-index-contrast ring core fiber," *J. Lightw. Technol.*, vol. 39, no. 2, pp. 600–611, Jan. 15, 2021.

[44] P. Gregg, P. Kristensen, A. Rubano, S. Golowich, L. Marrucci, and S. Ramachandran, "Spin-orbit coupled, non-integer OAM fibers: Unlocking a new eigenbasis for transmitting 24 uncoupled modes," in *Proc. Conf. Lasers Electro-Optics*, San Jose, CA, USA, Jun. 2016, pp. 1–2.

[45] F. A. Al-Zahrani and K. Ahmed, "Novel design of dual guided photonic crystal fiber for large capacity transmission in high-speed optics communications with supporting good quality OAM and LP modes," *Alexandria Eng. J.*, vol. 59, no. 6, pp. 4889–4899, Dec. 2020.

[46] M. M. Hassan, M. A. Kabir, M. N. Hossain, T. K. Nguyen, B. K. Paul, K. Ahmed, and V. Dhasarathan, "Numerical analysis of circular core shaped photonic crystal fiber for orbital angular momentum with efficient transmission," *Appl. Phys. B, Lasers Opt.*, vol. 126, no. 9, pp. 1–8, Sep. 2020.

[47] M. M. Hassan, M. A. Kabir, M. N. Hossain, B. Biswas, B. K. Paul, and K. Ahmed, "Photonic crystal fiber for robust orbital angular momentum transmission: Design and investigation," *Opt. Quantum Electron.*, vol. 52, no. 1, pp. 1–14, Jan. 2020.

[48] M. A. Kabir, K. Ahmed, M. M. Hassan, M. M. Hossain, and B. K. Paul, "Design a photonic crystal fiber of guiding terahertz orbital angular momentum beams in optical communication," *Opt. Commun.*, vol. 475, Nov. 2020, Art. no. 126192.

[49] M. F. Israk, M. A. Razzak, K. Ahmed, M. M. Hassan, M. A. Kabir, M. N. Hossain, B. K. Paul, and V. Dhasarathan, "Ring-based coil structure photonic crystal fiber for transmission of orbital angular momentum with large bandwidth: Outline, investigation and analysis," *Opt. Commun.*, vol. 473, Oct. 2020, Art. no. 126003.

[50] S. Li and J. Wang, "Multi-orbital-angular-momentum multi-ring fiber for high-density space-division multiplexing," *IEEE Photon. J.*, vol. 5, no. 5, Oct. 2013, Art. no. 7101007.

YINGNING WANG received the B.S. degree in electronic science and technology from Shandong University, Qingdao, China, in 2019. She is currently pursuing the M.S. degree in optical engineering with the Institute of Modern Optics, Nankai University, Tianjin, China.

WENQIAN ZHAO received the B.S. degree in applied physics from Shandong University, Weihai, China, in 2020. He is currently pursuing the M.S. degree in optical engineering with the Institute of Modern Optics, Nankai University, Tianjin, China.

WENPU GENG received the B.S. degree in optical information science and technology from Nankai University, Tianjin, China, in 2019, where she is currently pursuing the M.S. degree in optical engineering with the Institute of Modern Optics.

YUXI FANG received the bachelor's degree in optical information science and technology from Anhui University, Hefei, China, in 2018. She is currently pursuing the master's degree with the Institute of Modern Optics, Nankai University, Tianjin, China. Her research interest includes integrated optics.

CHANGJING BAO received the Ph.D. degree in electrical engineering from the University of Southern California, Los Angeles, CA, USA, in 2017. He has authored and coauthored more than 100 journal articles and conference proceedings. His research interests include optical communications, nonlinear optics, and integrated optics.

ZHI WANG received the Ph.D. degree in optics from Nankai University, Tianjin, China, in 2005. He is currently a Professor with the Institute of Modern Optics, Nankai University. His research interests include photonic crystal fiber/multimode fiber mode control theory, micro/nanostructured fiber sensing technology, ultrafast fiber laser technology, nonlinear fiber optics, and nonlinear space-time dynamics of multimode fiber.

HAO ZHANG received the Ph.D. degree in optics from Nankai University, Tianjin, China, in 2005. He is currently a Professor with the Institute of Modern Optics, Nankai University. His research interests include micro/nanostructured fiber devices, novel fiber sensors, and fiber lasers.

YONGXIONG REN received the B.E. degree in communications engineering from the Beijing University of Posts and Telecommunications (BUPT), Beijing, China, in 2008, the M.S. degree in radio physics from Peking University (PKU), Beijing, in 2011, and the Ph.D. degree in electrical engineering from the University of Southern California (USC), Los Angeles, CA, in 2016.

He has authored and coauthored more than 130 research articles with a Google Scholar citation number of >5500. His publications include 57 peer-reviewed journal articles, 76 international conference proceedings, one book chapter, and three patents. His research interests include high-capacity free-space and fiber optical communications, millimeter-wave communications, space division multiplexing, orbital angular momentum multiplexing, atmospheric optics, and atmospheric turbulence compensation.

ZHONGQI PAN (Senior Member, IEEE) received the B.S. and M.S. degrees in electrical engineering from Tsinghua University, China, and the Ph.D. degree in electrical engineering from the University of Southern California, Los Angeles.

He is currently a Professor with the Department of Electrical and Computer Engineering. He also holds the BORSF Endowed Professorship in electrical engineering II, and the BellSouth/BoRSF Endowed Professorship in telecommunications. He has authored/co-authored 160 publications, including five book chapters, 18 invited presentations/articles. He also has five U. S. patents and one China patent. His research interests include photonics, including photonic devices, fiber communications, wavelength-division-multiplexing (WDM) technologies, optical performance monitoring, coherent optical communications, space-division-multiplexing (SDM) technologies, and fiber sensor technologies. He is the OSA.

YANG YUE (Member, IEEE) received the B.S. and M.S. degrees in electrical engineering and optics from Nankai University, Tianjin, China, in 2004 and 2007, respectively, and the Ph.D. degree in electrical engineering from the University of Southern California, Los Angeles, CA, USA, in 2012.

He is currently a Professor with the Institute of Modern Optics, Nankai University. He has published over 200 peer-reviewed journal articles and conference proceedings, four edited books, one book chapter, >ten invited articles, >50 issued or pending patents, and >100 invited presentations. His current research interests include intelligent photonics, optical communications and networking, optical interconnect, detection, imaging and display technology, integrated photonics, free-space, and fiber optics.

Dr. Yue is a member of the IEEE Communications Society (ComSoc), the IEEE Photonics Society (IPS), the International Society for Optical Engineering (SPIE), the Optical Society of America (OSA), and the Photonics Society of Chinese-American (PSC). He is an Associate Editor for IEEE Access, and an Editor Board Member for three other scientific journals. He also served as Guest Editor for eight journal special issues, a Committee Member and the Session Chair for >50 international conferences, a Reviewer for >60 prestigious journals, and a Reviewer for OSA Centennial Special Events Grant 2016.